Journal Pre-proofs

Water sorption and hydration in spray-dried milk protein powders: selected physicochemical properties

Valentyn Maidannyk, David McSweeney, Sean A. Hogan, Song Miao, Sharon Montgomery, Mark Auty, Noel A. McCarthy

PII: S0308-8146(19)31532-8
DOI: https://doi.org/10.1016/j.foodchem.2019.125418
Reference: FOCH 125418

To appear in: *Food Chemistry*

Received Date: 31 January 2019
Revised Date: 1 August 2019
Accepted Date: 21 August 2019

Please cite this article as: Maidannyk, V., McSweeney, D., Hogan, S.A., Miao, S., Montgomery, S., Auty, M., McCarthy, N.A., Water sorption and hydration in spray-dried milk protein powders: selected physicochemical properties, *Food Chemistry* (2019), doi: https://doi.org/10.1016/j.foodchem.2019.125418

Water sorption and hydration in spray-dried milk protein powders: selected physicochemical properties

Valentyn Maidannyk, David McSweeney, Sean A. Hogan, Song Miao, Sharon Montgomery, Mark Auty, Noel A. McCarthy*.

Food Chemistry & Technology Department, Teagasc Food Research Centre, Moorepark, Co. Cork, Ireland.

*Corresponding author. Tel.: 00353 25-42205

E-mail address: noel.mccarthy@teagasc.ie

Keywords: Milk protein concentrate, vapour phase diffusion, lactose crystals, structural strength, glass transition, microstructure.

Abstract

Low and high protein dairy powders are prone to caking and sticking and can also be highly insoluble; with powder storage conditions an important factor responsible for such issues. The aim of this study is focused on the bulk and surface properties of anhydrous and humidified spray-dried milk protein concentrate (MPC) powders (protein content ~40, 50, 60, 70 or 80%, w/w). Water sorption isotherms, polarized light and scanning electron micrographs showed crystallized lactose in low protein powders at high water activities. High protein systems demonstrated increased bulk diffusion coefficients compared to low protein systems. Glass transition temperatures, α-relaxation temperatures and structural strength significantly decreased with water uptake. CLSM measurements showed that humidified systems have slower real time water diffusion compared to anhydrous systems. Overall, the rate of water diffusion was higher for low protein powders but high protein powders absorbed higher levels of water under high humidity conditions.

1. Introduction

Dairy protein powders are used in a wide variety of nutritional products as base formulations or as complete nutritional products. Low protein powders (skim milk) are exported globally and used extensively in fat filled products, as coffee whiteners, yogurts, etc. High protein dairy powders are often used as sole nutritional products (i.e., in muscle building and sports recovery products) but are also used in high value products (e.g., infant formulae) or for protein standardization in skim milk. Issues associated with dairy protein powders vary depending on protein/carbohydrate concentration and are usually as a result of prolonged storage under non-ideal environmental conditions. Low protein powders are susceptible to lactose crystallization under high humidity or temperature, compared to high protein powders which are relatively insoluble immediately after spray drying, with solubility deteriorating with storage (Agarwal et al., 2015). Dairy protein powders become more costly with increasing protein content due to the high associated capital and operational expenditure required to produce these ingredients (Marouli and Maroulis, 2005). After drying, powders are packaged under atmospheric conditions and transported worldwide often with little temperature control during storage. As such, the functional properties (flowability, wettability, dissolution, etc.) of these powders can be significantly affected (Felix da Silva et al., 2018).

Knowledge of the mechanisms involved in dairy powder hydration is limited, and new data is required to understand the key factors controlling the process. The hydration process may be divided into four main steps: wetting, swelling, dispersion and full hydration (Gaiani et al., 2007). One of the key processes occurring in amorphous powders during rehydration is effective water transfer in to particles. Water acts as a plasticizer and solvent, causing many changes in the bulk properties of high and low protein systems (Fan and Roos, 2016). However, little is known about the effect that the innate water content of powders has

on hydration at a molecular and microstructural level due to the complexity of powder constituents, shear forces and the level of water diffusion which is directly related to porosity (Murrieta-Pazos et al., 2011; Yuan et al., 2018). Other factors, such as product composition, degree of heat treatment during pasteurization and the viscosity of the liquid feed to the dryer all influence powder particle morphology, which subsequently affects powder rehydration properties (Kim et al., 2009).

Milk protein concentrate (MPC) powders are produced from skim milk using a combination of processing techniques, such as ultrafiltration (UF), evaporation and spray drying. UF is a membrane separation technology used to fractionate milk components based on molecular weight size. Therefore, skim milk can be fractionated in to two main streams through the retention of milk proteins and permeation of smaller molecular weight components such as lactose, minerals and non-protein nitrogen. Usually, freshly produced milk powders are in the unstable amorphous state directly after drying and it is important that this state is maintained during storage and transport (Roos and Drusch, 2015). Thermodynamically unstable amorphous powders can transform to a more stable phase under certain conditions. During this transformation, which occurs at a defined temperature (i.e., the glass transition temperature, T_g), amorphous systems (glassy state) exhibit critical changes to their physical properties, such as reduced viscosity, a reduction in structural relaxation time, increased molecular mobility and are converted to supercooled liquids (e.g. rubbery state) with time-dependent flow (Angell, 2002; Maidannyk, 2017). These changes can cause serious deterioration to product quality, such as cake hardening, reduced powder flowability, increased powder free fat and insolubility, etc. (Fan and Roos, 2017; Felix da Silva et al., 2018).

However, there are a number of analytical methods to determine the critical temperature and water content at which these changes occur. Structural strength concept

combines changes in temperature T_α-T_g or T-T_g, as a function of time (critical change in structural relaxation time) (Roos, 2013). This approach has been applied successfully to a number of different food systems, such as carbohydrate-protein matrices, miscible carbohydrate systems, partially crystalline and encapsulated systems (Fan and Roos, 2016, 2017; Maidannyk and Roos, 2016, 2017, 2018; Maidannyk et al., 2017, 2019). However, the structural strength concept has not previously been used to characterize spray-dried dairy protein powders. A number of well-established methods are available that examine water absorption in powders, such as T_g (Kelly et al., 2015) and water sorption isotherms (Murrieta-Pazos et al., 2011; Yuan et al., 2018). Perry and Green (1984) examined the effective bulk diffusivity by analysis of water sorption data in systems stored under saturated salt solutions (Rizvi, 1986). Dynamic mechanical analysis (DMA) in a multi-frequency mode is a common method used to determine the α-relaxation temperature (T_α), which usually occurs at ~20-30°C above the calorimetric T_g. Therefore, by measuring the T_α of a system it can predict the initiation of structural changes in amorphous powders prior to reaching the T_g. While, a relatively new method published by Maidannyk et al. (2019b) has used confocal laser scanning microscopy (CLSM) to determine real time diffusion of water in to dairy powders. Previous studies (Biliaderis et al. 2002; Chivrac et al., 2010; Forny et al., 2011; Roos and Drusch, 2015; Fan and Roos, 2017; Felix da Silva et al., 2018) have shown the significant role of water content in powder stability and product shelf-life. However, the relationship between initial water content and subsequent rehydration properties of dairy powders has not been addressed. Issues remain for food companies trying to formulate nutritional products using high protein dairy powders while maintaining acceptable hydration properties. Identifying the optimum powder composition to satisfy both the end-user needs in terms of nutritional profile and user experience is important with this study highlighting the expected powder properties across a wide range of protein contents. The main hypothesis of

this research was to identify the critical parameters involved in powder hydration across a range of dairy protein systems in order to predict product deterioration.

Therefore, the main purpose of the current study was to investigate the effect of water on the physical properties, such as water sorption, glass transition, α-relaxation temperature, structural strength, crystallization, morphology and real time water diffusion in dairy protein powders.

2. Materials and Methods

2.1. Materials

MPC powders were produced in the Bio-functional Food Engineering Facility at Teagasc Food Research Centre (Moorepark, Fermoy, Co.Cork). Concentrated milk permeate (~21%, w/w, total solids (TS) content) and milk protein concentrate (~21% TS; 83%, w/w, protein content) were supplied by a local dairy company. A total of five powders were produced by recombining liquid milk permeate to the milk protein concentrate in order to produce four samples containing protein contents of ~40, 50, 60 and 70% (w/w) along with the milk protein concentrate obtained directly from the commercial UF plant i.e., 80%, w/w, protein. All samples (MPC 40, 50, 60, 70 and 80) were allowed to equilibrate overnight at 4 °C under gentle agitation. Each batch (15 Kg) was pre-heated to a temperature of ~45 °C and dried using a single-stage spray dryer equipped with a two-fluid nozzle atomization system. Air inlet and outlet temperatures were set at 185 and 80 °C, respectively. Table 1 shows the macro composition of all the MPC powders produced

2.2. Determination of the initial water content (IWC)

All MPC powder samples (0.5-1.0 g) were dried at 70 °C at an absolute pressure of <10 mbar for 24 h in a Jeio Tech OV-12 vacuum oven (Jeio Tech®, Seoul, Korea) in order to

determine the initial water content (IWC). The difference in mass of samples before and after drying (g/100g of dry solids) was defined as the initial water content.

2.3. Water sorption analysis

Vacuum-dried MPC powders were stored in a desiccator over P_2O_5 until further analysis. Each powder was stored in an evacuated desiccator (21 ± 2°C) for 12 days over saturated solutions of LiCl, CH_3COOK, $MgCl_2$, K_2CO_3, $Mg(NO_3)_2$, $NaNO_2$, NaCl and KCl (Sigma Chemical Co., St. Louise, MO. U.S.A.), which when equilibrium was reached provided 0.11, 0.23, 0.33, 0.44, 0.545, 0.66, 0.76 and 0.85 water activity (a_w), respectively. The a_w of each powder was measured using a Novasina, Labmaster.aw (Novatron, London, UK). During storage of the powders under different relative humidities samples were weighed at time points of 0, 2, 4, 6, 8, 10, 24, 48 and 72 h and then every 24 h up to 144 h. The water content in each system was plotted as a function of time, and the Guggenheim-Anderson-de Boer (GAB) relationship was fitted to data to relate a_w and powder water content (Maidannyk et al., 2019) (Eq. 1):

$$\frac{m}{m_0} = \frac{Cka_w}{(1 - ka_w)(1 - ka_w + Cka_w)} \quad (1)$$

where m is the water content (g of water/100 g of dry solids), m_0 - the monolayer value of water content, C, k - constants related to energy constant, which are calculated from m_0.

2.4. Particle size distribution and morphology

The particle size distribution (in %), circularity, convexity and elongation of anhydrous and humidified (RH values of 0, 11, 23, 33, 44, 54.5, 65, 76 and 85%) MPC powders was obtained using a Malvern Morphologi G3 (Malvern Instruments, Malvern, UK) image analysis-based particle characterization system (Maidannyk et al., 2019).

2.5. Determination of bulk diffusion coefficient

Water kinetics profiles were used to calculate the effective bulk diffusivity. Based on the assumption that water sorption is limited by diffusion, the solution of Fick's second law equation for a one-dimensional slab can be obtained as shown in Eq. 2 (Murrieta-Pazos et al., 2011).

$$\Gamma = \frac{(\mathrm{M} - \mathrm{Me})}{(\mathrm{Mo} - \mathrm{Me})} = \frac{8}{(\Pi)^2}\sum_{n=0}^{\infty}(2n+1)^{-2}\exp\frac{Deff(2n+1)^2\,(\Pi)^2 t}{4L^2} \quad (2)$$

where M_e is equilibrium moisture content, M_o is initial moisture content, M is moisture content at time t, L = thickness of the slab. This equation assumes that the initial moisture content is uniform and that surface moisture and density remain constant. Equation 3 was used to determine the effective or apparent diffusion (Rizvi, 1986).

$$Deff = -\left(\frac{4L^2}{\Pi^2}\right) * Slope \quad (3)$$

The slope is determined from a plot of Ln(Γ) versus time. When a break in this plot is observed, diffusion coefficients can be determined for each part of the curve (Rizvi, 1986).

2.6. Differential Scanning Calorimetry (DSC)

Differential scanning calorimetry, DSC (Q200, TA instruments, DE U.S.A.), was used to measure the T_g of amorphous MPC 40-80 powders after storage at 0, 0.11, 0.23, 0.33 and 0.44 a_w. Each sample was transferred to pre-weigh standard DSC aluminium pans (40 µL, Tzero Hermetic Lid, TA instruments, Switzerland) and hermetically sealed. An empty pan was used as a reference. For anhydrous systems, the lids of DSC aluminium pans were

punctured to allow evaporation of residual water upon the measurement. All samples were scanned from 30 °C below the T_g to 30 °C above at a heating rate of 5 °C/min, before cooling back to the initial starting temperature at a rate of 10 °C/min. Subsequently, a second heating scan was performed to 50 °C above the T_g at a heating rate of 5 °C/min. The onset of T_g was determined from the second heating step using the TA Universal Analysis software (TA instruments, DE U.S.A.).

2.7. Dynamical Mechanical Analyses (DMA)

DMA (Q800, TA instruments, DE, U.S.A.) was used to measure mechanical properties (E″ – loss modulus, E′ – storage modulus and tan δ = E″'/E′) of anhydrous and humidified MPC powders (as described in Section 2.6). The DMA instrument was calibrated to determine the zero displacement position before measurements were performed. Sample were analysed by placing approximately 0.2 g of powder on a metal pocket-forming sheet, which was fixed inside a dual cantilever. All results were obtained using the TA Universal Analysis software. Samples were scanned from ~ 50°C below to 50°C over the α-relaxation at a heating rate of 1°C/min and cooling rate of 5°C/min, using the dual-cantilever bending mode. T_α values were determined from peak of tan δ above the glass transition (Maidannyk et al., 2017).

To calculate the relaxation times (τ) of peak T_α, as a function of frequency (f), Equation 4 was used (Maidannyk, 2017):

$$\tau = \frac{1}{2\pi f} \tag{4}$$

2.8. Calculation of Williams Landel Ferry (WLF) model constants and the structural strength parameter

To calculate the structural strength parameter (S), the constants C_1 and C_2 from Williams Landel Ferry (WLF) equation were obtained, as described by Roos and Drusch (2015). The WLF equation was used to fit DMA data (Eq. 5):

$$log_{10}\frac{\tau}{\tau_s} = log_{10}\frac{\eta}{\eta_s} = \frac{-C_1(T-T_g)}{C_2+(T-T_g)} \quad (5)$$

where, τ is relaxation time, τ_s is reference relaxation time, η is viscosity, η_s is reference viscosity, T is temperature, T_g is glass transition temperature, C_1 and C_2 are constants.

The WLF equation in the form of (Eq. 6) suggested that the plot of $1/lg(\tau/\tau_s)$ versus $1/(T-T_g)$ gives a linear correlation:

$$\frac{1}{lg\frac{\tau}{\tau_s}} = \frac{1}{-C_1} - \frac{C_2}{C_1(T-T_g)} \quad (6)$$

The WLF constants C_1 and C_2 were derived from the slope and interception (Roos and Drusch, 2015).

Mathematically, structural strength is based on WLF relationship and can be calculated by Equation (7):

$$S = \frac{dC_2}{C_1 - d} \quad (7)$$

where d is a parameter, showing the critical decrease in the number of logarithmic decades for the flow (e.g., 100 to 0.01 s corresponds to $d = 4$; can be chosen for each system as an

integer depending on the critical time for the process), C_1 and C_2 are "non-universal" constants in the WLF equation.

Equation 8 was used to predict structural strength as a function of water content:

$$S = \frac{w_1 S_1 + k w_2 S_2}{w_1 + k w_2} \quad (8)$$

where w_1 – weight fraction of dry solid; w_2 – weight fraction of water; k – coefficient; S_1 – structural strength for anhydrous system; S_2 – structural strength of pure water (S_2 = 6.0) (Maidannyk et al., 2017).

2.9. Microstructure

2.9.1. Polarized light microscopy

Anhydrous and humidified MPC 40 - 80 powders were examined using an Olympus BX51 (Olympus Corporation, Tokyo, Japan) light microscope with 20x dry objective lens with polarized light. Digital images (TIFF, 8-bit) were taken and captured using a Jenoptik C14 Imagic camera. All systems were analysed pre- and post-lactose crystallization following water uptake after storage over saturated salt solutions at different relative humidities. Crystallized lactose appeared as bright areas under polarized light (Maher et al., 2015).

2.9.2. Confocal laser scanning microscopy (CLSM)

A Leica TCS SP5 CLSM (Leica Microsystems CMS GmbH, Wetzlar, Germany) was used for visualization of powder particles and determination of real-time diffusion coefficients for MPC 40, MPC 60 and MPC 80 powders equilibrated at 0, 33 and 65% RH. The method was based on the real-time visualisation of 0.1%, w/w, Rhodamine B (Sigma-Aldrich Co., St. Louise, MO. U.S.A.) dissolved in milli-Q water penetrating into individual

anhydrous and humidified MPC powder particles using the DPSS 561 nm laser. The diffusion process was slowed down using polyethylene glycol (PEG) with 1:0, 1:1, 1:3 and 1:4 rhodamine to PEG ratios, so as to retard rapid water uptake. Confocal images were taken using a 63x oil immersion objective with a numerical aperture of 1.4. The 2-D area of powder particles was measured by Image Pro Premier 3D software and subsequently z-stacks were obtained in order to generate a 3-D structure of the particles. Green, pseudo-coloured pictures (8-bit), 512x512 pixels in size, were acquired using a zoom factor of 1 - 3. Real-time effective diffusivity values were obtained from analysis of CLSM pictures, as described by Maher et al. (2015) and Maidannyk et al. (2019).

2.9.3. Scanning electron microscopy

Powders were attached to double-sided adhesive carbon tabs mounted on scanning electron microscope stubs, and coated with chromium (K550X, Emitech, Ashford, UK). Scanning electron microscopy images were taken using a Zeiss Supra 40P field emission SEM (Carl Zeiss SMT Ltd., Cambridge, UK) at 2.00 kV. Representative micrographs were taken at 200×, 500×, 1000×, 5000× and 10000× magnification (Maidannyk et al., 2019).

2.10. Data analysis

All experiments were performed in triplicate. Mean results of water sorption, DSC and DMA analyses were calculated from three replicates with standard deviations expressed as error bars. One-way analysis of variance (ANOVA) was applied to compare means of data (water sorption, glass transition, structural strength and effective diffusivity) using SPSS software (IBM SPSS Statistics version 24). Means were considered significantly different at $p < 0.05$.

3. Results and discussion

3.1. Water sorption analysis

Water sorption profiles of MPC 40, 50, 60, 70 and 80 powders measured at different RH values are shown in Fig. 1. All systems show typical water sorption behaviour for amorphous powders from 11 to 54.5% RH (Fig. 1). At RH values >54.5%, powders with a protein content greater than 50%, w/w, continued to absorb water; however, for MPC40 and 50 powders a decrease in the water content was observed, indicating lactose crystallisation above a a_w of 0.55 and 0.85, respectively. The higher a_w required to crystallize lactose in MPC50 and the fact that lactose in MPC60 to 80 powders did not undergo crystallization may be due to the preferential sorption of water by protein which hindered the rate at which lactose underwent the change from the 'glassy' to the 'rubbery' phase. Hogan and O'Callaghan (2010) found similar results for low protein skim milk powders which were stored at RH values from 10 to 66%. In the present study, the high protein content in MPC60-80 powders may have also hindered the mobility of lactose molecules to reorganise in to the crystalline form. However, after powders were allowed to equilibrate for 144 h, it was observed that as the level of protein in powders increased so did the amount of water absorbed, irrespective of lactose crystallization (Table S1). GAB sorption isotherms (lines) and experimental data (symbols) for non-crystalline MPC 40 - 80 powders are shown in Fig. S1. The GAB model shows a good fit to experimental data for MPC 60 - 80 over the entire water activity range studied. However, for MPC 40 and MPC 50 powders stored at high water activity values (i.e., $\geq$ 0.55 a_w) the GAB curve showed much higher water content, compared to the experimental data (Fig. S1), due to the occurrence of lactose crystallization in MPC40 and 50 powders. This is in agreement with many authors, who used the GAB equation to model water sorption data for lactose and other low protein dairy powders (McCarthy et al., 2013; Maidannyk and Roos, 2017).

Apparent effective moisture (vapor phase) diffusivity (D_{eff}), measured as a function of relative humidity at 21°C, is shown in Fig. S2. Results in the present study are based on the assumption that water sorption kinetics are limited only by diffusion and that D_{eff} is constant for each RH and an average particle size is applied to all particles (Murrieta-Pazos et al., 2011). Systems containing a high protein content (i.e., MPC 60 – 80) showed a bell-shaped behaviour while MPC 40 and 50 systems showed increasing D_{eff} up to RH values of 44 and 55%, which is in agreement with previous reports (Chivrac et al., 2010; Roca et al., 2008; Murrieta-Pazos et al., 2011). The bell-shaped curve observed for high protein MPC powders may by explained as follows: at low RH, water sorption occurs rapidly as lactose in the amorphous state is hygroscopic and absorbs moisture readily. However, as the a_w of the system increases and plasticization commences the propensity for crystalline lactose to absorb water decreases significantly, leading to a decrease in diffusivity, with similar results found by Murrieta-Pazos et al. (2011) for whole milk and skim milk powders. For high lactose containing systems, the average surface area is significantly higher than for high protein containing systems, which results in increasing D_{eff} from RH 11% to 44% (Fig. S2). However, at 55% RH the D_{eff} decreased due to the occurrence of lactose crystallization. Lactose in the crystalline state has a lower D_{eff} capacity compared to in the amorphous state, which is in agreement with the free volume theory for polymers (Yuan et al., 2018; Palzer, 2010).

3.2. Glass transition temperature of milk protein powders

The onset of calorimetric glass transition temperature of anhydrous and humidified MPC 40 - 80 systems was measured from the second heating step in DSC thermographs. T_g values for all powders are shown in Table S2 and Fig. S3. Anhydrous powders with protein concentrations of 60, 70 and 80%, w/w, showed slightly higher T_g values compared to lower

protein systems (MPC40 and 50), due to the high molecular weight of protein molecules. These results are in agreement with previous studies (Maidannyk and Roos, 2016, 2017; Shamblin et al., 1996; Biliaderis et al., 2002; Haque and Roos, 2004), which showed that the addition of protein increases the T_g value of carbohydrates (lactose, trehalose, sucrose). The T_g values of all MPC powders significantly ($P < 0.05$) decreased with increasing water content (Table S2 and Fig. S3), irrespective of the protein concentration, indicating that the system was plasticized during water absorption (Silalai and Roos, 2011). Therefore, glass transition occurred in and closely followed only the carbohydrate (lactose) component of the systems across the entire water activity range studied (Maidannyk and Roos, 2017).

3.3. Dynamic-mechanical properties

Structural α-relaxation occurred in amorphous systems at temperatures between 20-30°C and above the onset of the calorimetric T_g (Table S3). For anhydrous and humidified MPC 40 – 80 systems, T_α values were obtained from the peak temperature of dynamic tan δ (tan δ = E''/E', where E'' is the loss modulus (mechanical energy dissipation), E' is the storage modulus (mechanical energy storage)) obtained from dynamic mechanical analyses. DMA spectra are frequency-dependent, allowing for the relaxation time-temperature dependence of amorphous systems to be obtained (Eq. 3) (Silalai and Roos, 2011; Maidannyk, 2017; Fan and Roos 2016, 2017; Maidannyk and Roos, 2016, 2017, 2018). Systems with higher protein content showed significantly broadened and less intensive DMA peaks compared to high lactose systems (results not shown). Also these systems showed slightly higher T_α, which could be caused by proteins acting as a physical barrier hindering the molecular mobility of amorphous lactose (Fan and Roos, 2016; Maidannyk and Roos, 2016). Water is an effective plasticizer and can increase the free volume of systems as well as molecular mobility of amorphous matrices (Royall et al., 2005; Meinders and van Vliet,

2009) which in this study resulted in the significant ($P < 0.05$) decrease in T_α for all MPC powders (Table S3). This result is in agreement with many previous studies (Silalai and Roos, 2011, Fan and Roos 2016, 2017; Maidannyk and Roos, 2016, 2017, 2018) which examined the effects of protein content in mixed carbohydrate systems.

3.4. Williams Landel Ferry modelling and structural strength

The WLF model, with "non-universal" constants, is commonly used to describe the temperature dependence of viscosity and structural relaxation time. C_1 and C_2 constants were calculated by assuming that viscosity and structural relaxation time of supercooled liquids are approaching 10^{12} Pa.s and 100 s, respectively. However, upon heating, viscosity and relaxation time values can decrease to ~10^5 Pa.s and 10^{-14} s, respectively, as described in numerous studies (Angell, 2002; Roos, 2013; Fan and Roos 2016, 2017; Maidannyk and Roos, 2016, 2017, 2018; Maidannyk et al., 2017, 2019). Table S4 shows the WLF constants for anhydrous and humidified MPC40 - 80 powders from which structural strength was calculated using Equation 7. Powders containing high protein content showed greater structural strength behaviour compared to low protein powders (Fig. S4), as low protein powders were more susceptible to water plasticization (Table S5, Fig. S4), with ~23°C temeprature difference between anhydrous MPC40 and MPC80 systems (Table S5, Fig. 2a). This is in agreement with previous data shown for trehalose- and lactose-whey protein isolate systems (Maidannyk and Roos, 2016 and 2017). Structural strength increased linearly with increasing protein content in powders (Fig. S5a) and correspondingly decreased with increasing lactose concentration (Fig. S5b). This trend was independent of water content and can help predict the structural strength of multicomponent protein powders as a function of water content.

Structural strength is a parameter which enables direct comparison of structural relaxation times of powders in the vicinity of and above the T_g (Roos, 2013). Fig. 2 shows experimental data derived from DMA and DSC profiles (symbols) and modified WLF curves (lines). During heating, a critical and significant change in structural relaxation time occurred between 10^{-2} and 10^{2} s (Fig. 2a). Table S5 shows data for S, which was calculated at d = 4. Using Equation 8 the structural strength was correlated with water content for each powder and the relationship was applied to MPC40 – 80 powders and produced models with good fit (Fig. S4). The *k* value was 7.1±1.8, 6.1±1.3, 5.7±1.5, 5.4±1.8 and 4.9±1.7 with 75.2, 78.6, 74.6, 66.7 and 68.1% goodness of fit for MPC40, 50, 60, 70 and 80, respectively.

3.5. Microstructure

3.5.1. Polarized light microscopy (PLM) and scanning electron microscopy (SEM)

PLM was carried out on anhydrous (RH 0%) and humidified (RH 54.5%) MPC40, 60 and 80 systems and is shown in Fig. 3. No lactose crystals were observed in any of the anhydrous powders. However, PLM images of powders stored at 54.5% RH showed significant observable differences compared to their anhydrous counterparts. Humidified MPC40 showed that lactose crystals formed in the bulk and on the surface of the powder particles (Fig. 3b), as was also seen by water sorption data in Fig. 1. MPC60 powders (Fig. 3d) showed a small number of isolated crystals which were located just under the particle surface, while MPC80 powders (Fig. 3f) contained no observable lactose crystals.

SEM images of anhydrous (Fig. 4a, c, e, g, i) and humidified (after 144 h at RH 54.5%) (Fig. 4b, d, f, h, j) MPC powders are shown in Fig. 4. The surface microstructure of MPC 40 - 80 powders significantly differed, depending on powder composition. Anhydrous systems with high lactose content showed a collapsed structure with a “shrivelled-like” surface composed of shallow folds (Fig. 4a and c), while high protein systems showed more

regular, spherical particles with a relatively smooth surface (Fig. 4e, g and i). These results are in agreement with many previous authors who showed similar results for anhydrous skim milk and milk protein powders (Murrieta-Pazos et al., 2011 and Kim et al., 2009; McCarthy et al., 2013). There were no significant differences in particle size and surface microstructure between anhydrous and humidified systems for MPC 50-80 powders (Fig. 4d, f, h and j). For these systems, anhydrous and humidified powder surfaces appeared smooth with only a few indentations, similar to previous data shown for dairy spray-dried powders (Hogan et al., 2001; Maher et al., 2015; McCarthy et al., 2013). However, the surface properties of humidified MPC 40 powder particles showed needle like "tomahawk" lactose crystals (Fig. 4b), which confirmed that lactose transformed from the amorphous metastable state to the more stable crystalline state at 54.5% RH. Interestingly, SEM images of humidified MPC50 did not show the needle-like crystal structures and is in-line with the water sorption profiles shown in Fig. 1, where lactose crystallization did not occur until storage at 85% RH.

3.5.2. Morphology and particle size distribution

Average particle size of anhydrous and humidified MPC 40-80 powders are shown in Table S6 and Fig. S6. Particle sphericity, convexity and elongation showed very little change with increasing water content for MPC 60 - 80 powders. However, at RH $\geq$ 54.5% the sphericity and elongation of MPC 40 and 50 significantly ($P < 0.05$) decreased due to the growth of lactose crystals, which is in agreement with water sorption data, SEM and PLM observations. The average powder particle diameters of MPC 60 - 80 increased only slightly with increasing water content in the system. While, for MPC 40 and MPC 50 powders, particle size increased and correlated with water uptake between RH 11 and 44%, and may be attributed to particle swelling due to water migration into the amorphous matrix. However, there was a decrease in particle size around RH 54.5% due to the collapse of the amorphous

matrix (lactose/protein) triggered by lactose crystallization. Again, particle size increased at RH >76% due to powder caking, which is in agreement with previous works (Silalai and Roos, 2010; Murrieta-Pazos et al., 2011). Therefore, powders with high lactose content had the highest swelling properties compared to powders with more protein, where particles showed almost humidity-independent behaviour, which was similar to results obtained in previous work by Maidannyk et al. (2019).

3.6. Real time liquid phase diffusion

Confocal scanning microscopy (CLSM) images are shown in Fig. S7. Mixtures of rhodamine B and PEG 200 at different ratios (1:4; 1:3 and 1:1) were added to anhydrous and humidified (RH 33% and 65%) MPC40, 60 and 80 powders, which allowed for diffusion of the dye molecules into the particles, but prevented solubilization and changes to particle morphology. Images taken at fixed time intervals represent real-time water diffusion into powder particles. Particle diameters were determined using Leica TCS SP5 software in the range of 3 to 100 μm. Initially, powders appeared as dark particles against a dark green background. During the water diffusion process, fluorescent dye penetrated into particles resulting in them becoming a bright green colour (Fig. S7). Water diffusion rate occurred quickest for small particles as shown in Fig. S7, with the D_{eff} coefficients increasing linearly with increasing particle size (results not shown). Forny et al. (2011) showed similar results in commercial powders whereby smaller particles absorbed water faster than larger particles.

The initial water content of the powders prior to water diffusion significantly affected ($P < 0.05$) the effective real time diffusivity of low protein/high lactose powders (MPC40), while no affect was observed for high protein powders (Fig. 5). For example, in the case of MPC40 powder the effective diffusivity decreased from 3×10^{-11} m^2/s in the anhydrous state to 5×10^{-12} m^2/s when humidified at RH 65%, while for MPC 80 systems changes were not

significant (from 4×10^{-13} to 2×10^{-13} m^2/s). This can be explained by lactose crystallisation in the bulk and on the surface of MPC40 powders, compared to MPC 60 and 80 powders where sorption, swelling and caking occurred. The data obtained by CLSM showed that for liquid phase the values of D_{eff} are lower than for vapour phase by several orders of magnitude, with the highest value of liquid phase D_{eff} observed in MPC 40 due to higher solubility of the non-protein constituents, as described by Crowley et al. (2015). However, in the vapour phase D_{eff} was higher in high protein systems over the complete RH range studied (Fig. S2). This is possibly due to the large differences between the transport of liquid and vapour water.

4. Conclusion

The hydration of dairy protein powders is significantly affected by protein:lactose ratio, as is the rate of deterioration in powder functionality during storage. High protein powders are highly insoluble compared to high lactose powders but are not as susceptible to lactose crystallization. Once amorphous lactose in dairy powders has undergone crystallization their hydration ability decreases. However, measuring the α-relaxation temperature of powders was identified as a good indicator of an increase in molecular mobility and onset of plasticization. Low and high protein powders also differed in terms of the rate between liquid and vapour phase diffusion. This study has identified and highlighted that there exists a critical balance between protein:lactose ratio to obtain acceptable hydration properties and good shelf-life, and is dependent on ingredient composition and environmental conditions, allowing nutritional companies to make informed decisions during product development.

5. Acknowledgments

This work was supported by the Food Institutional Research Measure (FIRM) project "Developing the next generation of high protein spray dried dairy powders with enhanced hydration properties" (15-F-679) funded by the Department of Agriculture, Food and Marine, Teagasc Food Research Centre, Moorepark, Co. Cork, Ireland.

6. References

Agarwal, S., Beausire, R. L., Patel, S., & Patel, H. (2015). Innovative uses of milk protein concentrates in product development. *Journal of Food Science, 80(S1),* A23-A29.

Angell, C., (2002). Liquid fragility and the glass transition in water and aqueous solutions. *Chemical reviews 102(8),* 2627-2650.

Biliaderis, C., Lazaridou, A., Mavropoulos, A. and Barbayiannis, N. (2002). Water plasticization effects on crystallization behavior of lactose in a co-lyophilized amorphous polysaccharide matrix and its relevance to the glass transition. *International Journal of Food Properties 5 (2):* 463-482.

Chivrac, F., Angellier-Coussy, H., Guillard, V., Pollet, E., & Avérous, L. (2010). How does water diffuse in starch/montmorillonite nano-biocomposite materials?. *Carbohydrate Polymers, 82(1),* 128-135**.**

Crowley, S. V., Desautel, B., Gazi, I., Kelly, A. L., Huppertz, T., & O'Mahony, J. A. (2015). Rehydration characteristics of milk protein concentrate powders. *Journal of Food Engineering, 149,* 105-113.

Fan, F., & Roos, Y. H. (2016). Structural relaxations of amorphous lactose and lactose-whey protein mixtures. *Journal of Food Engineering, 173*, 106-115.

Fan, F., & Roos, Y. H. (2017). Glass transition-associated structural relaxations and applications of relaxation times in amorphous food solids: a review. *Food Engineering Reviews, 9(4)*, 257-270.

Felix da Silva, D., Ahrné, L., Ipsen, R., & Hougaard, A. B. (2018). Casein-Based Powders: Characteristics and Rehydration Properties. *Comprehensive Reviews in Food Science and Food Safety, 17(1*), 240-254.

Forny, L., Marabi, A., & Palzer, S. (2011). Wetting, disintegration and dissolution of agglomerated water soluble powders. *Powder Technology, 206(1)*, 72-78.

Gaiani, C., Boyanova, P., Hussain, R., Pazos, I. M., Karam, M. C., Burgain, J., & Scher, J. (2011). Morphological descriptors and colour as a tool to better understand rehydration properties of dairy powders. *International Dairy Journal, 21(7)*, 462-469.

Haque, M.K. and Roos, Y., (2004). Water Plasticization and Crystallization of Lactose in Spray-dried Lactose/Protein Mixtures. *Journal of Food Science 69 (1)*: FEP23-FEP29.

Hogan, S. A., McNamee, B. F., O'Riordan, E. D., & O'Sullivan, M. (2001). Microencapsulating properties of sodium caseinate. *Journal of Agricultural and Food Chemistry, 49(4),* 1934-1938.

Hogan, S. A., & O'Callaghan, D. J. (2010). Influence of milk proteins on the development of lactose-induced stickiness in dairy powders. International Dairy Journal, 20(3), 212-221.

Kelly, G. M., O'Mahony, J. A., Kelly, A. L., Huppertz, T., Kennedy, D., & O'Callaghan, D. J. (2015). Influence of protein concentration on surface composition and physico-chemical properties of spray-dried milk protein concentrate powders. *International Dairy Journal, 51,* 34-40

Kim, E. H. J., Chen, X. D., & Pearce, D. (2009). Surface composition of industrial spray-dried milk powders. 3. Changes in the surface composition during long-term storage. *Journal of food engineering, 94(2),* 182-191.

Maher, P. G., Auty, M. A. E., Roos, Y. H., Zychowski, L. M., & Fenelon, M. A. (2015). Microstructure and lactose crystallization properties in spray dried nanoemulsions. *Food Structure, 3*, 1-11.

Maidannyk, V. (2017). Strength analysis for understanding structural relaxations in food materials. PhD thesis. University College Cork.

Maidannyk, V., Roos, Y., (2016). Modification of the WLF model for characterization of the relaxation time-temperature relationship in trehalose-whey protein isolate systems. *Journal of Food Engineering 188,* 21-31.

Maidannyk, V. A., Roos, Y. H. (2017). Water sorption, glass transition and "strength" of lactose–Whey protein systems. *Food Hydrocolloids, 70,* 76-87.

Maidannyk, V. A., Nurhadi, B., Roos, Y. H. (2017). Structural strength analysis of amorphous trehalose-maltodextrin systems. *Food Research International, 96,* 121-131.

Maidannyk, V. A., Roos, Y. H. (2018). Structural strength analysis of partially crystalline trehalose. *LWT-Food Science and Technology, 88,* 9-17.

Maidannyk V., Lutjes E., Montgomery S., Mc.Carthy N., Auty M. (2019). Measurement of effective diffusion coefficients in dairy powders by confocal microscopy and sorption kinetic profiles. *Food Structure, 20,* 100108.

Maidannyk, V. A., Lim, A. S. L., Auty, M. A. E., & Roos, Y. H. (2019). Effects of lipids on the water sorption, glass transition and structural strength of carbohydrate-protein systems. *Food Research International, 116,* 1212-1222.

Marouli, A. Z., & Maroulis, Z. B. (2005). Cost data analysis for the food industry. *Journal of food Engineering, 67(3)*, 289-299.

McCarthy, N. A., Gee, V. L., Hickey, D. K., Kelly, A. L., O'Mahony, J. A., & Fenelon, M. A. (2013). Effect of protein content on the physical stability and microstructure of a model infant formula. *International Dairy Journal, 29(1),* 53-59.

Meinders, M. B., van Vliet, T., (2009). Modeling water sorption dynamics of cellular solid food systems using free volume theory. *Food Hydrocolloids 23(8),* 2234-2242.

Murrieta-Pazos, I., Gaiani, C., Galet, L., Cuq, B., Desobry, S., & Scher, J. (2011). Comparative study of particle structure evolution during water sorption: skim and whole milk powders. *Colloids and Surfaces B: Biointerfaces, 87(1)*, 1-10.

Palzer, S. (2010). The relation between material properties and supra-molecular structure of water-soluble food solids. *Trends in Food Science & Technology, 21(1),* 12-25.

Perry, R. H., Green, D. W., & Maloney, J.O. (1984). Perry's chemical engineers' handbook., 6th ed. McGraw Hill, New York.

Rizvi, S. S., (1986). Thermodynamic properties of foods in dehydration. *Engineering properties of foods, 2,* 223-309.

Roca, E., Broyart, B., Guillard, V., Guilbert, S., & Gontard, N. (2008). Predicting moisture transfer and shelf-life of multidomain food products. *Journal of Food Engineering, 86(1),* 74-83.

Roos, Y. H., (2013). Relaxations, glass transition and engineering properties of food solids, Advances in Food Process Engineering Research and Applications. Springer, pp. 79-90.

Roos, Y. H., Drusch, S., (2015). Phase transitions in foods. *Academic Press.*

Royall, P. G., Huang, C.-y., Tang, S.-w.J., Duncan, J., Van-de-Velde, G., Brown, M.B., (2005). The development of DMA for the detection of amorphous content in pharmaceutical powdered materials. *International journal of pharmaceutics 301(1),* 181-191.

Silalai, N. and Y. H. Roos (2011). Mechanical relaxation times as indicators of stickiness in skim milk–maltodextrin solids systems. *Journal of Food Engineering 106 (4):* 306-317.

Shamblin, S.L., Huang, E.Y. and Zografi, G., (1996). The effects of co-lyophilized polymeric additives on the glass transition temperature and crystallization of amorphous sucrose. *Journal of thermal analysis 47 (5):* 1567-1579.

Yuan, L., Lu, L. X., Chen, Y. H., & Pan, L. (2018). Moisture diffusion model of two-component food under different contact conditions in impermeable package. *Heat and Mass Transfer,* 1-9.

Figures

Figure 1. Water sorption kinetics for milk protein concentrate 40 (a), 50 (b), 60 (c), 70 (d) and 80 (e) powders at different relative humidity's 11, 23, 33, 44, 55, 65, 76, 85%, measured over 144 h at 21±2°C.

Figure 2. Modified WLF curves (lines) and experimental data (symbols) for MPC 40 – 80 powders after equilibration for 144 h at relative humidity's of 0 (a), 11 (b), 23 (c), 33 (d) and 44% (e) at 25±1°C.

Figure 3. Light (a, c, e) and polarized light (crossed polars) micrographs of MPC 40 (a, b), MPC 60 (c, d) and MPC 80 (e, f) anhydrous (a, c, e) and after storage for 144 h at 54.5% humidity (b, d, f), scale bar = 100 μm.

Figure 4. Scanning electron micrographs of milk protein concentrate 40 (a, b), 50 (c, d), 60 (e, f), 70 (g, h) and 80 (i, j) powders in anhydrous form (column 1) and after storage for 144 h at 54.5% humidity (column 2). Arrows indicate lactose crystals. Scale bars = 2μm.

Figure 5. Effective diffusivity as a function of water activity of MPC 40, 60 and 80 powders after storage for 144 h at 21°C.

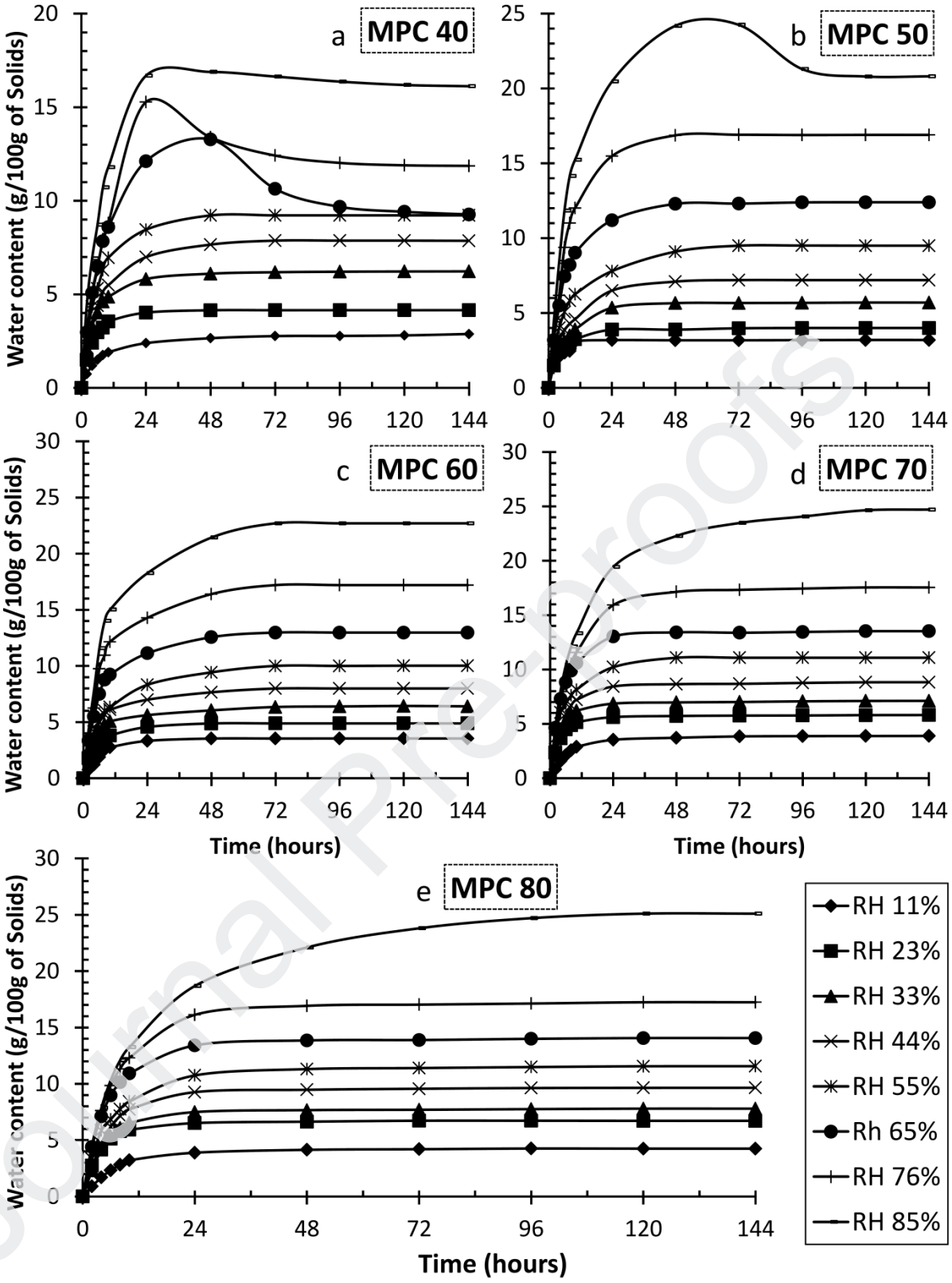

Figure 1.

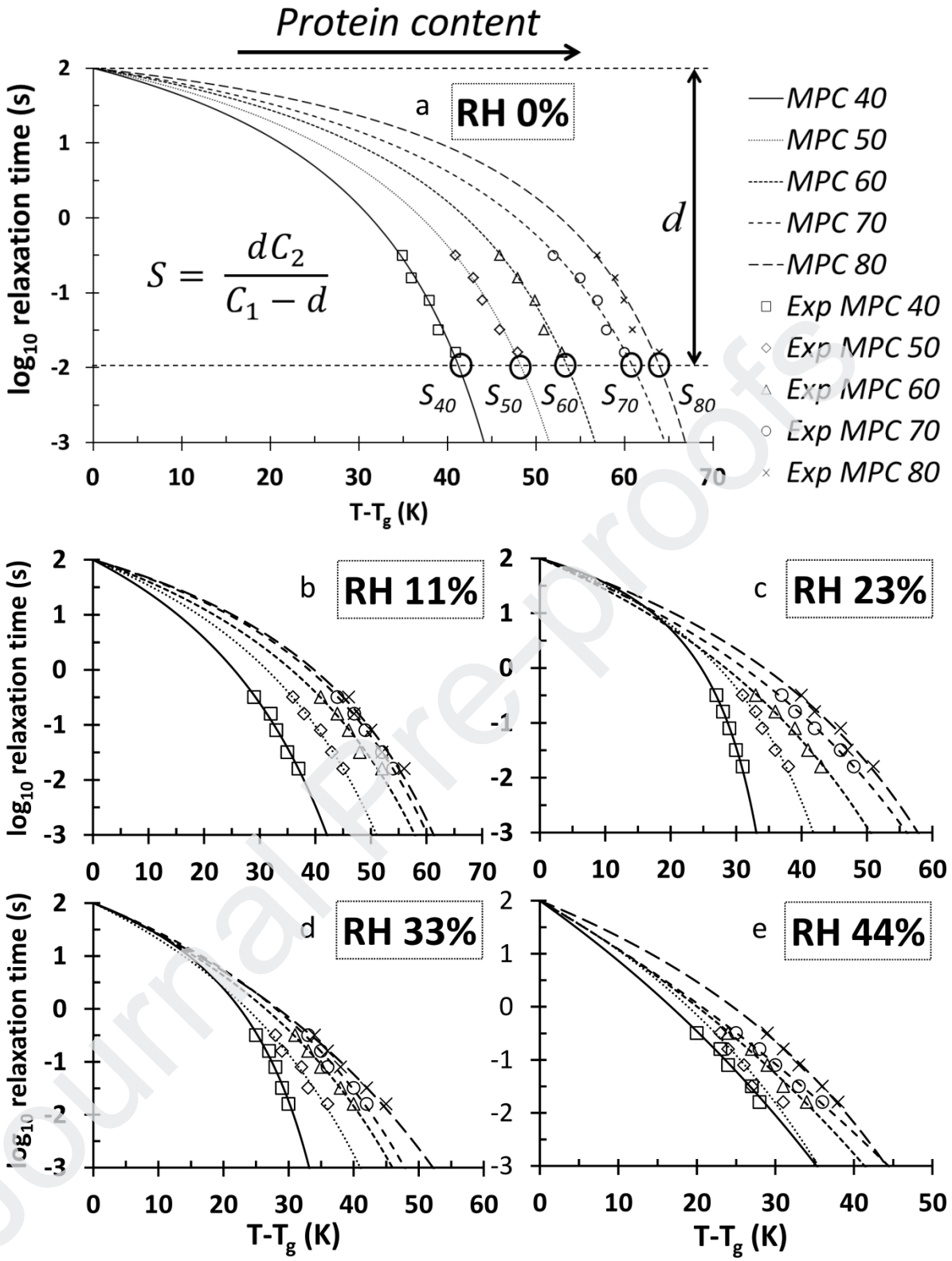
Protein content
a
RH 0%
b
RH 11%
c
RH 23%
d
RH 33%
e
RH 44%
MPC 40
MPC 50
MPC 60
MPC 70
MPC 80
Exp MPC 40
Exp MPC 50
Exp MPC 60
Exp MPC 70
Exp MPC 80
$S = \frac{dC_2}{C_1 - d}$
d
S_{40}
S_{50}
S_{60}
S_{70}
S_{80}
log10 relaxation time (s)
T-Tg (K)

Figure 2.

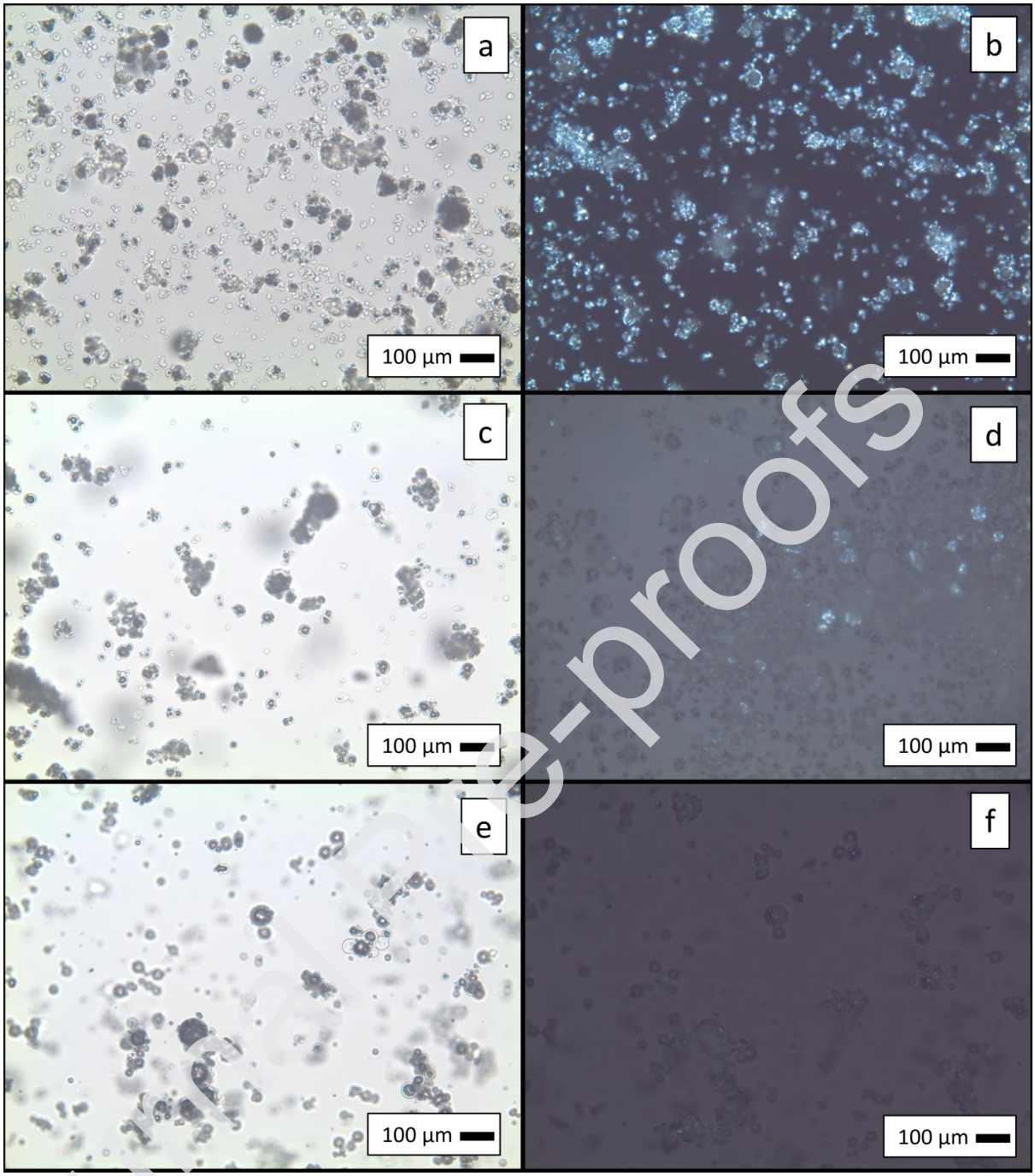

Figure 3.

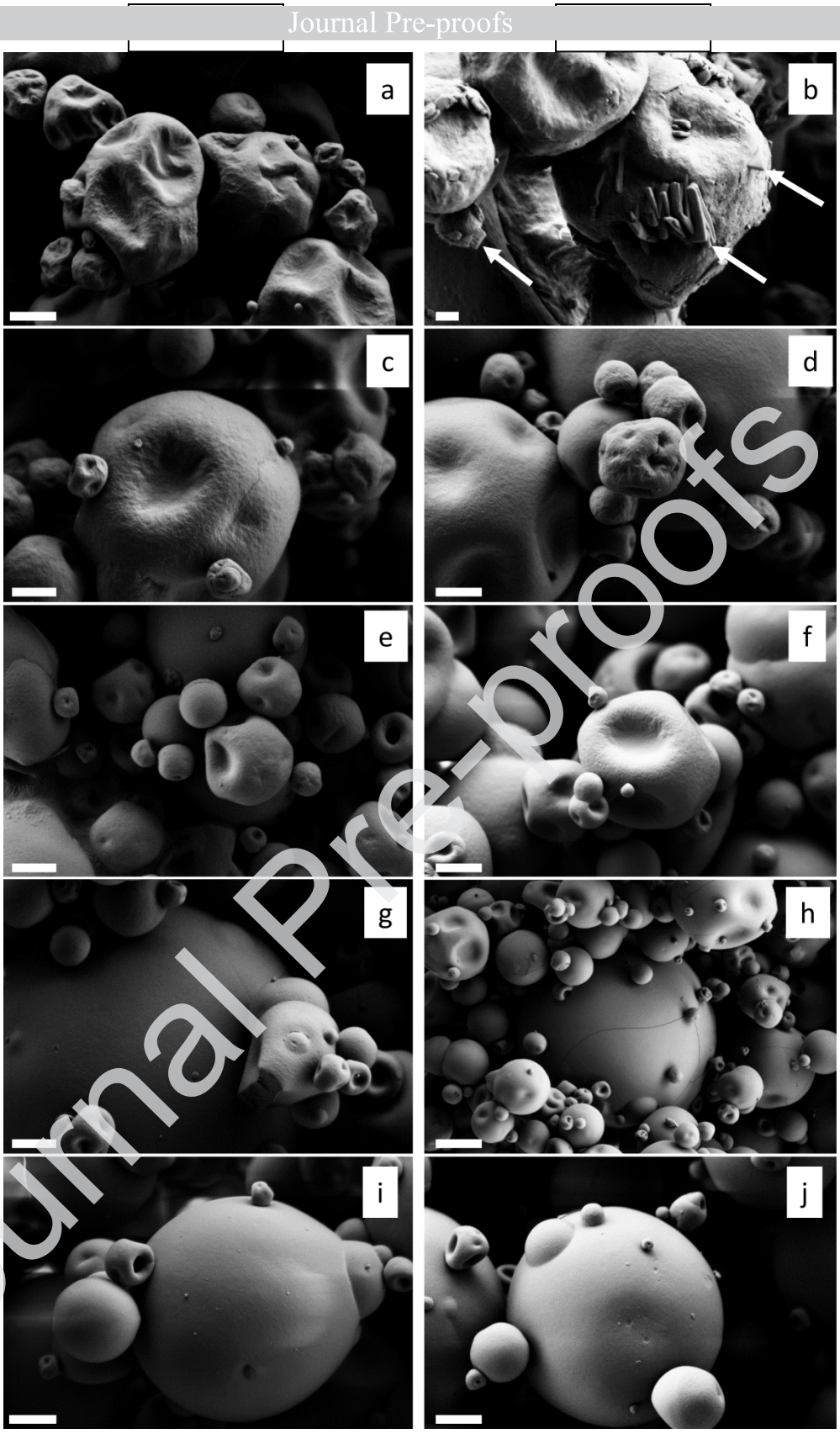

Figure 4.

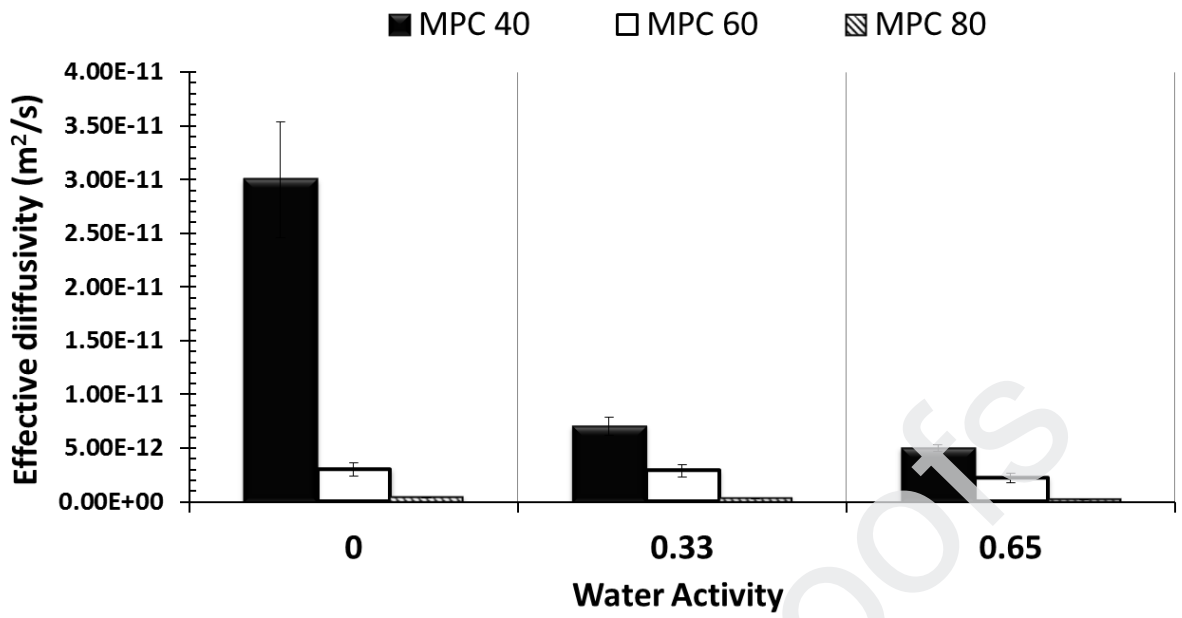

Figure 5.

Table 1. *Composition (g/100g of solids) of milk protein concentrate powders.*

Product	Lactose	Protein	Ash	IWC[a]
MPC 40	51.0 ± 4.0	39.0 ± 2.3	6.2 ± 2.1	4.1 ± 1.5
MPC 50	36.2 ± 5.1	52.1 ± 3.3	6.7 ± 2.1	4.1 ± 1.1
MPC 60	26.3 ± 3.8	63.3 ± 3.2	7.0 ± 2.2	4.4 ± 0.9
MPC 70	16.4 ± 2.8	71.1 ± 5.4	7.2 ± 2.3	5.7 ± 1.2
MPC 80	6.2 ± 2.3	81.2 ± 5.8	7.6 ± 2.3	5.2 ± 1.3

MPC: Milk protein concentrate

[a]IWC: Initial Water Content

- Powder water absorption rates were determined at different relative humidity
- High protein powders absorbed more water compered to low protein systems
- Water diffusion rates occurred slower in powders with high protein content

- Increasing relative humidity reduced powder particle strength
- Lactose crystallization occurred in low protein powders at high humidity